PSAA
READ 2024
RESEARCH & EDUCATION IN AIRCRAFT DESIGN
WARSAW, POLAND | 6-8 NOVEMBER 2024
POLITECHNIKA WARSZAWSKA
WARSAW UNIVERSITY OF TECHNOLOGY

Experimental assessment of Crashworthiness Capability of thin-walled CFRP tubes: using filament winding to enhance the energy absorption efficiency

T. Scalici[1], D. Tumino[1], G. Catalanotti[1] & A. Alaimo[1]*

[1]Kore University of Enna - Department of Engineering and Architecture, 94100, Enna (EN), Italy

*Corresponding author

Abstract

In the last decade, the use of fiber-reinforced composite materials has had a disruptive impact on the efficiency of both primary and low load-bearing structures for aerospace applications. The growing need to reduce CO2 emissions has led to a deep reconsideration of traditional materials in favour of a gradual yet unstoppable replacement across all components, including crashworthy structures. However, in this case, the energy absorption behaviour of composites cannot be reduced to plasticization phenomena but is driven by a wide set of factors mainly governing the formation of crack surfaces. For this reason, the design process may be more challenging.

In this work, a custom-built desktop filament winder was used to manufacture thin-walled tubes to be tested in axial compression. The unique layer architecture of the composite tubes used to produce the composite tubes was compared to a baseline, and an enhancement of the energy absorption capability was observed, thus suggesting a new route to follow for improving the performance of this class of structures.

Keywords: Crashworthiness, Filament winding, CFRPs, Thin-walled tubes

1. Introduction

The safety and integrity of a vehicle's occupants during a violent event, such as a crush or impact, depend on the structure's ability to absorb and dissipate energy from the collision, thus reducing the risk of injuries and fatalities. In recent years, this concept has been particularly emphasized and studied, especially in the automotive sector. However, numerous examples of energy-absorbing structures exist across various fields, including aeronautics (e.g., energy-absorbing elements beneath the seats to mitigate the effects of deceleration in the event of accidents).

Traditionally, metal structures have been used as energy absorbers due to the ability of this class of materials to absorb a significant amount of energy through plastic deformation. In contrast, composites function differently. In this case, the creation of crack surfaces, matrix and fiber fractures, fiber pull-out, debonding, and delamination are the primary mechanisms that contribute to energy dissipation [1].

The complexity of the failure behavior of fiber-reinforced polymers (FRPs) illustrates the challenges associated with designing crashworthy structures. Nevertheless, proper design, considering all the factors affecting crush behavior, can lead to substantial benefits in the application of FRPs in such contexts [2].

In general, an impact structure should be designed to absorb impact energy, withstand impact loads, and ensure a smooth deceleration. To achieve these three goals during a crush test, it is desirable to obtain high peak loads, a mean crush force that is not significantly different from the peak loads, and progressive failure that allows for controlled deceleration. Regarding the last point, researchers often utilize an edge chamfer as a triggering mechanism [3]. However, studies have shown inconsistent results concerning the effect of trigger geometry on Specific Energy Absorption (SEA) during dynamic crushing [4].

In this work, the authors propose an approach based on material architecture to be applied in tubular crush structures to promote progressive failure and enhance crushing properties. To manage the material structure throughout the manufacturing process, various techniques, such as fiber placement and pultrusion, can be explored. However, due to the tubular configuration of the crushing structures and their intended application, filament winding was chosen as the most suitable method. For this purpose, a desktop filament winder was developed and constructed to create thin-walled tubes. Cylindrical specimens were subjected to axial compression testing, and the resulting failure mechanisms were analyzed.

Results showed that introducing a bounding outer composite mesh can be considered a promising approach to improving the crashworthiness of composite energy-absorbing structures.

2. Materials & Methods

2.1 Custom-built desktop filament winder

Given the tubular shape of the sample selected for the experimental campaign, filament winding was considered the most suitable and efficient technique for producing lab-scale specimens. Therefore, a desktop filament winder was designed and built, with the prototype shown in Figure 1, where all the components are indicated. In this version, stepper motors are mounted on an aluminum frame. One motor control the rotation of the collecting mandrel, while the other controls the movement of the carriage (i.e., the aluminum structure that supports the carbon fiber spool, the resin pot, and the delivery head), which is guided by two sliders. The electronic control unit is connected to a computer via USB, and a commercial CNC software is used to control the path.

A G-code is generated using a MATLAB-based script that allows for designing the stacking sequence of the tubes, as described in the following paragraphs.

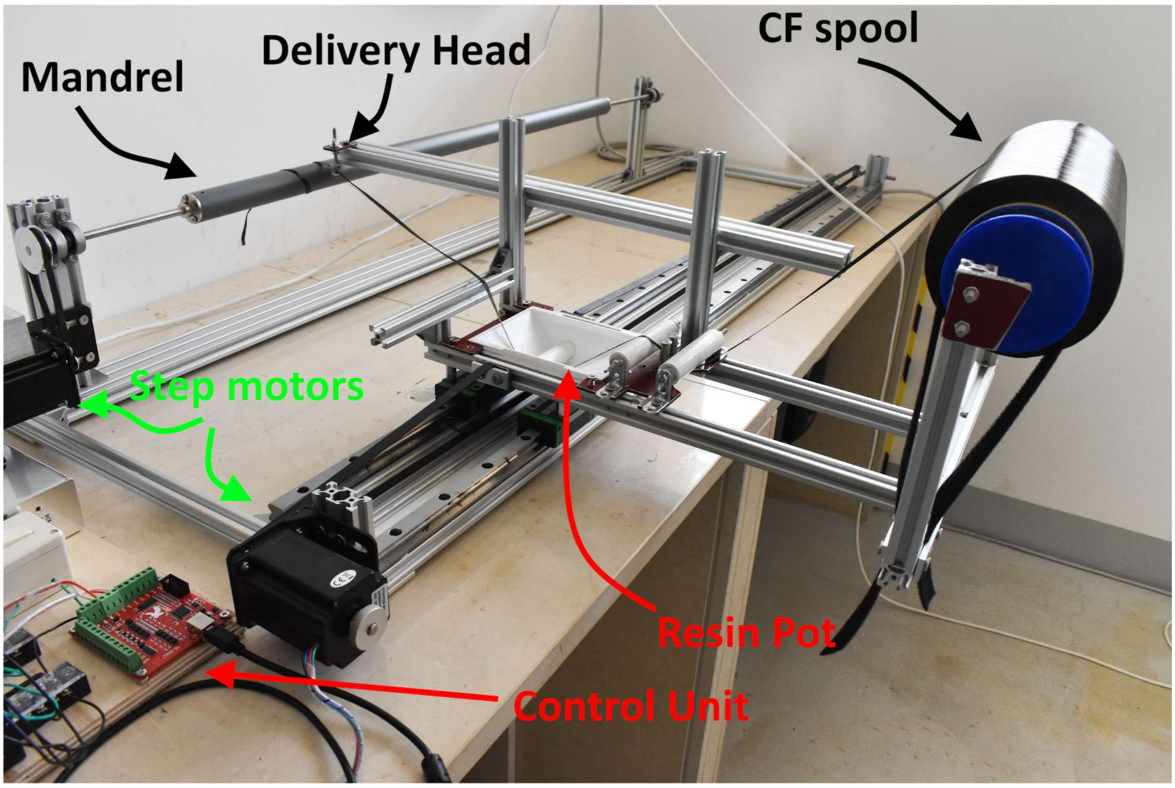

Figure 1 - Desktop filament winder

2.2 Composite Tubes and testing

Composite tubes, each 400 mm in length with an inner diameter of 32 mm, were manufactured using the equipment described in Section 2.1 following a wet winding process. Table 1 reports information on the resulting geometry. As the base material, two-layers composite tubes with a winding angle of 45° were manufactured for comparison purposes.

In the first modification (1st assembly), a ±60° carbon mesh was wound before the curing process, ensuring continuity between the base material and the reinforcing layer. For the second modification (2nd assembly), the base material was cured first, and then a ±60° carbon fiber mesh was added in a subsequent step, with a 25 µm PP layer interleaved to create a discontinuity.

As a reinforcement, a Mitsubishi Pyrofil TR 50S 6k PAN Carbon fiber tow, yielding a 400 TEX, with a nominal modulus of 235 GPa and tensile strength of 4410 MPa was used **Errore. L'origine riferimento non è stata trovata.**. The resulting dry areal weight of the reinforcement was $300\ g/m^2$. The resin used was an IN2 low-viscosity epoxy, provided by Easycomposite (UK)[6].

The maximum pattern number was chosen in the context of this experimental campaign as schematically shown in Figure 2.

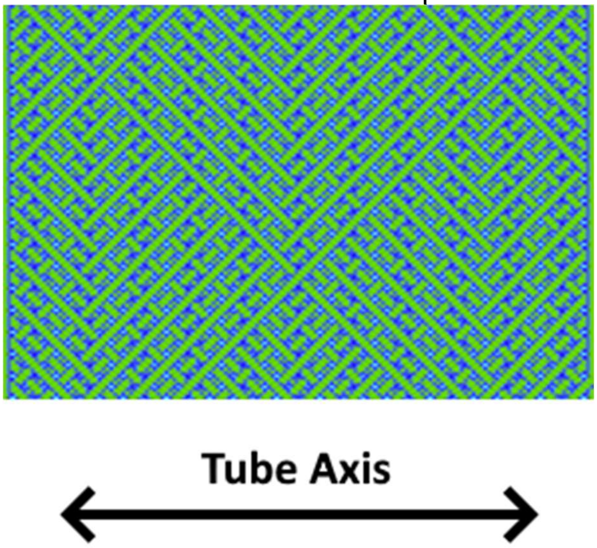

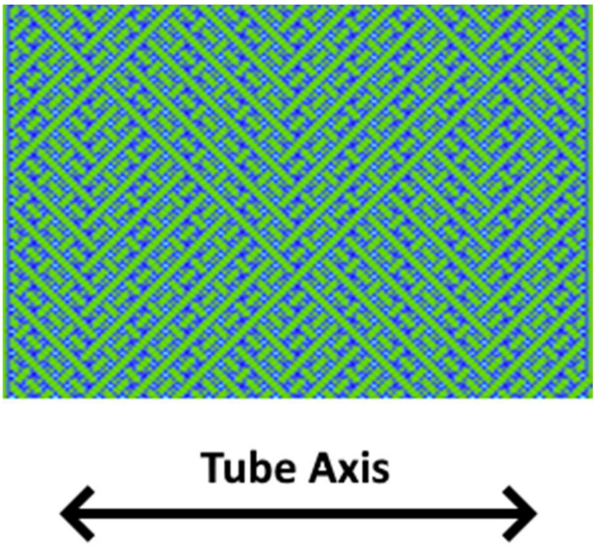

Figure 2 – Schematic representation of the winding pattern of the base material

Table 1 - Characteristics of the composite tubes

ID	Thickness [mm]	Layers	Winding angle [deg]	Linear weight [g]
Baseline	1.0	2	[45/45]	~120
1° Assembly (A*)	1.25	2.5	[45/45//60]	~130
2° Assembly (CC)	1.25	2.5	[45/45/PP/60]	~140

Samples with a nominal length of 80 mm were obtained from the tubes using a dry-cutting diamond saw. A lathe was used to machine the top and bottom surfaces of the cylinders, ensuring planarity.

Axial compression tests were conducted using an MTS Universal testing machine equipped with a 50 kN load cell, with a displacement rate of 20 mm/min. The crosshead displacement and reaction force were recorded directly by the machine software. All tests were stopped at a displacement of 50 mm. Given the low result scattering, a minimum of three samples were tested for each set.

Relevant crush parameters were obtained according the following equations:

$$E = \int F d\delta \rightarrow \boldsymbol{SEA} = \frac{E}{m} \quad (1)$$

$$\bar{P} = \frac{E}{\Delta\delta} \quad (2)$$

$$\eta = \frac{\bar{P}}{\mathrm{P_{max}}} \quad (3)$$

Where:

- E is the absorbed energy
- F is the registered reaction force
- SEA stand for Specific absorbed energy
- m is the nominal crushing mass corresponding to a length of 50mm
- $\bar{P}$ is the mean crushing force
- $\Delta\delta$ is the crushing displacement calculated after the first load drop
- $\mathrm{P_{max}}$ is the peak load
- η is defined as crushing efficiency

For the sake of clarity, a typical Force vs displacement curve is shown in Figure 3.

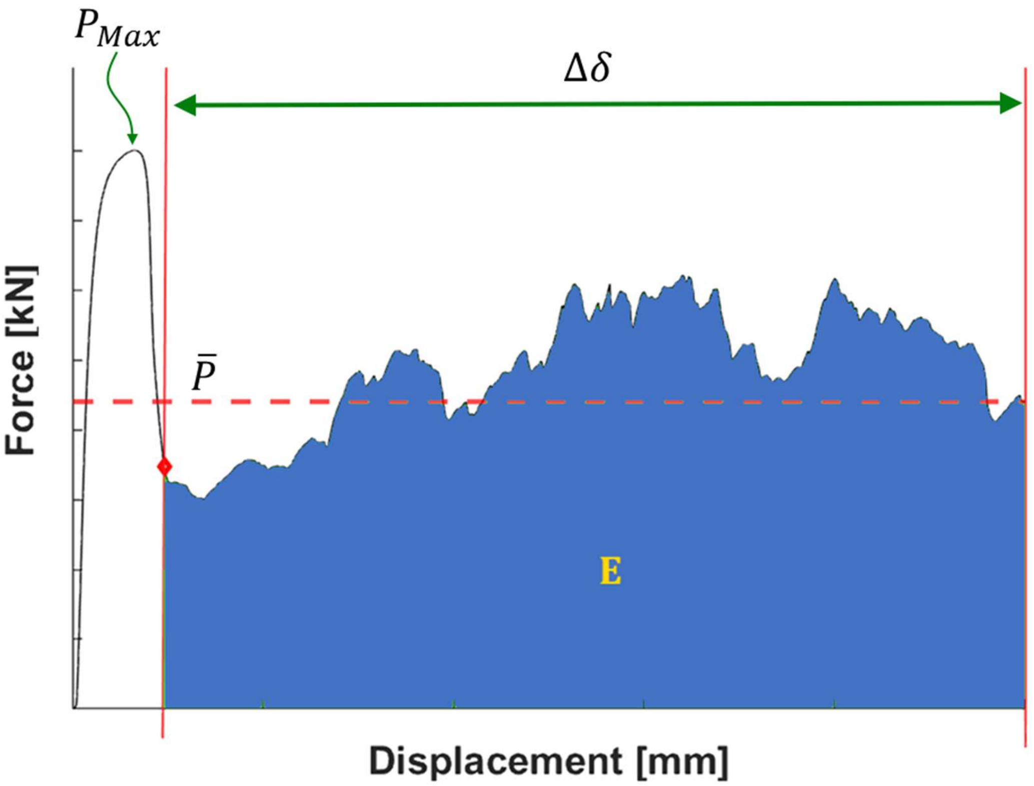

Figure 3 - Typical force vs. Displacement curve

3. Results and discussion

Figure 4 shows the typical force vs Displacement curves obtained by testing the baseline, 1st assembly and 2nd assembly samples, respectively. From the analysis of these results, it is possible to observe a significant increase of the peak force in the two cases when the bounding 60° mesh is present. This behaviour is more pronounced when the mesh is co-cured with the base material since the continuity promote the hooping role of the mesh during the compression resulting in a higher axial strength (~+107%). In the case of the 2nd assembly, this effect is still visible even if the discontinuity tends to mitigate the contribution of the external layer (~+75%). Figure 5 reports the numerical values of the mean peak forces in the three cases including the 95% confidence interval.

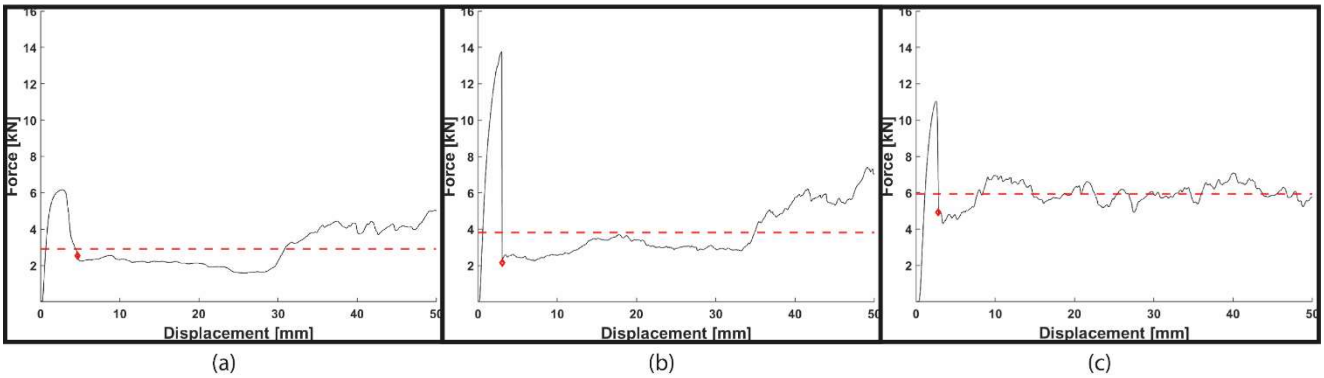

Figure 4 – Typical Force vs. Displacement Curves obtained from (a) Baseline, (b) 1st assembly and (c) 2nd assembly

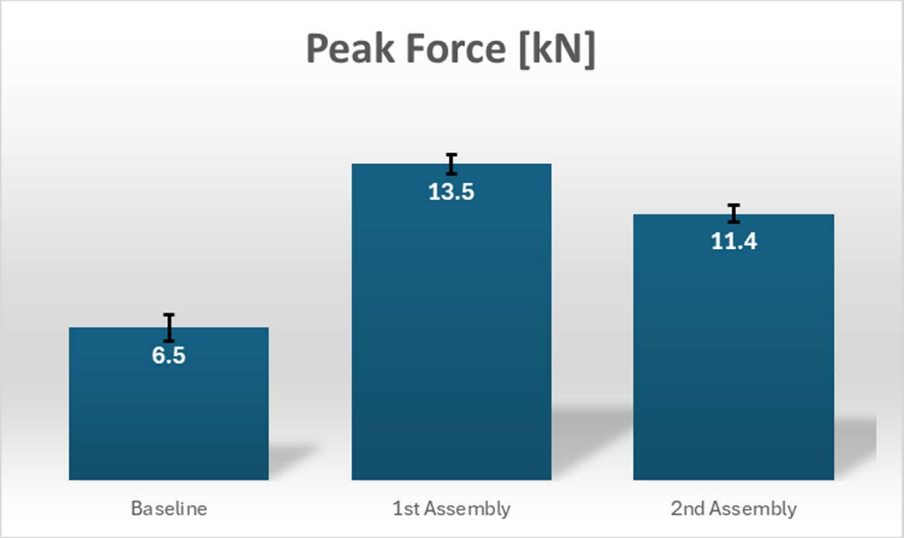

Figure 5 - Peak forces (average values - 95% C.I.)

The above hypotheses can be more clearly confirmed by analyzing the front and top views of the post-mortem samples shown in Figure 6. The baseline samples were characterized by failure behavior dominated by local instability, followed by wall kinking and subsequent fracture, resulting in a clearly visible localized fracture approximately in the mid-transverse plane (note: in general, the fracture position may vary depending on the actual condition of the sample, including defects or voids). A similar behavior was observed in the case of the 1st assembly, where the continuity between the base tube and the external 60° mesh does not allow significant differences in the failure modes to be seen when compared to the baseline. In this case, the mesh is generally forced to follow local out-of-plane displacements caused by buckling phenomena, limiting its contribution to a significant increase in hoop strength. Furthermore, in this case, mesh failure coincides with the catastrophic failure of the structure and a sudden drop in the reaction forces registered in Figure 4 (b).

In terms of crashworthiness, the beneficial effect of the mesh when separated from the base material by a release film can be observed in both in Figure 4 and Figure 6. Indeed, in Figure 4, a higher value of the mean crush stress is highlighted (red dotted lines). Additionally, the crush force tends to fluctuate with minor deviations around this value. The curves referring to the 2nd assembly lack the drops and rises in reaction force, which, on the other hand, are visible in the other cases due to structural instability, elastic energy storage, and its sudden release when failure occurs. In other words, the samples of the 2nd assembly fail progressively.

The effect of this failure mode can be seen in Figure 6, where the outer 60° mesh is still visible and maintains some integrity, even though it is clearly crushed. Nevertheless, its containment function was successfully fulfilled by promoting the progressive failure of the main bearing portions of the assembly and contributing to the increase of peak force by hooping the tubes.

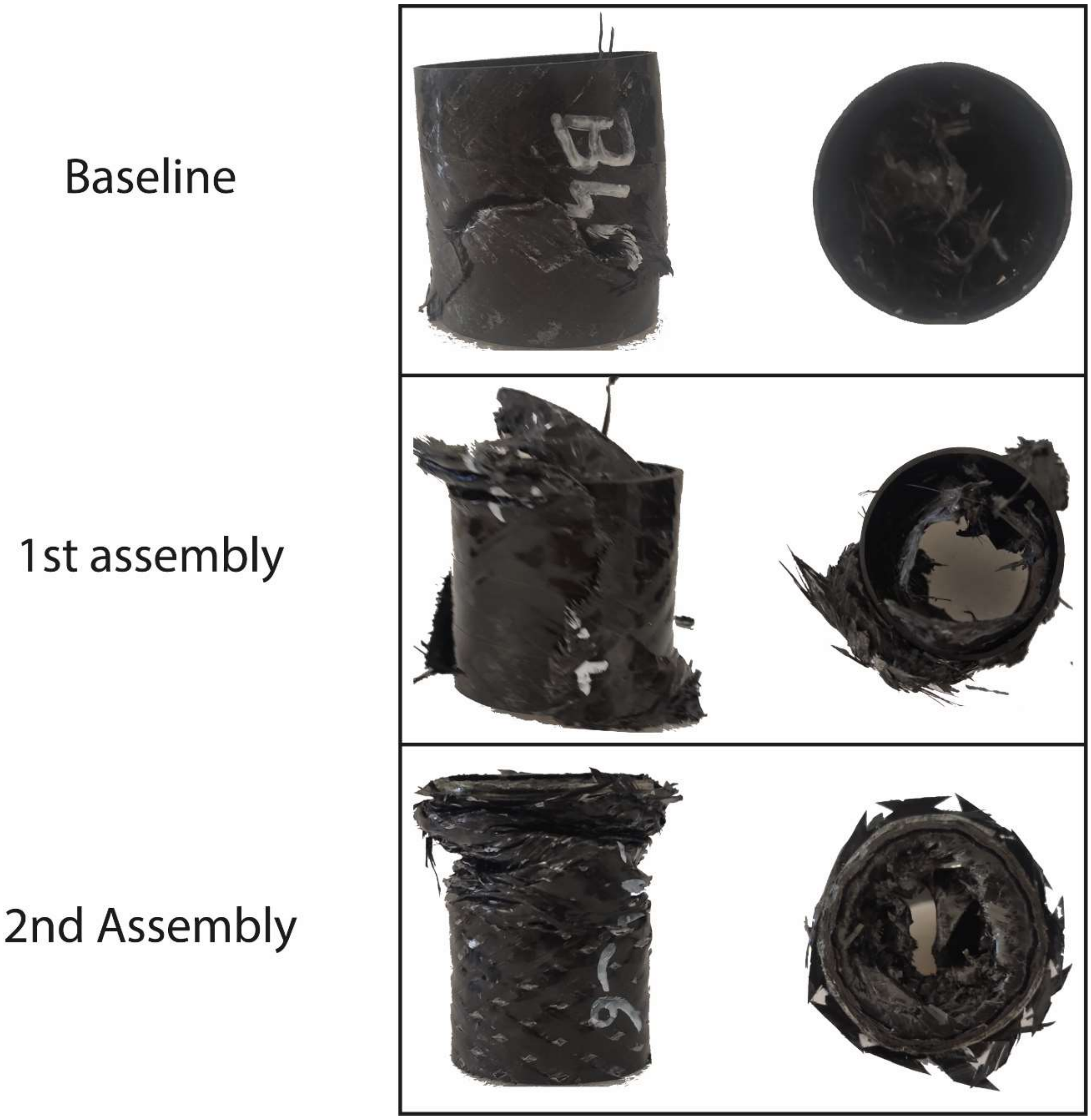

Figure 6 - Post-Mortem Samples

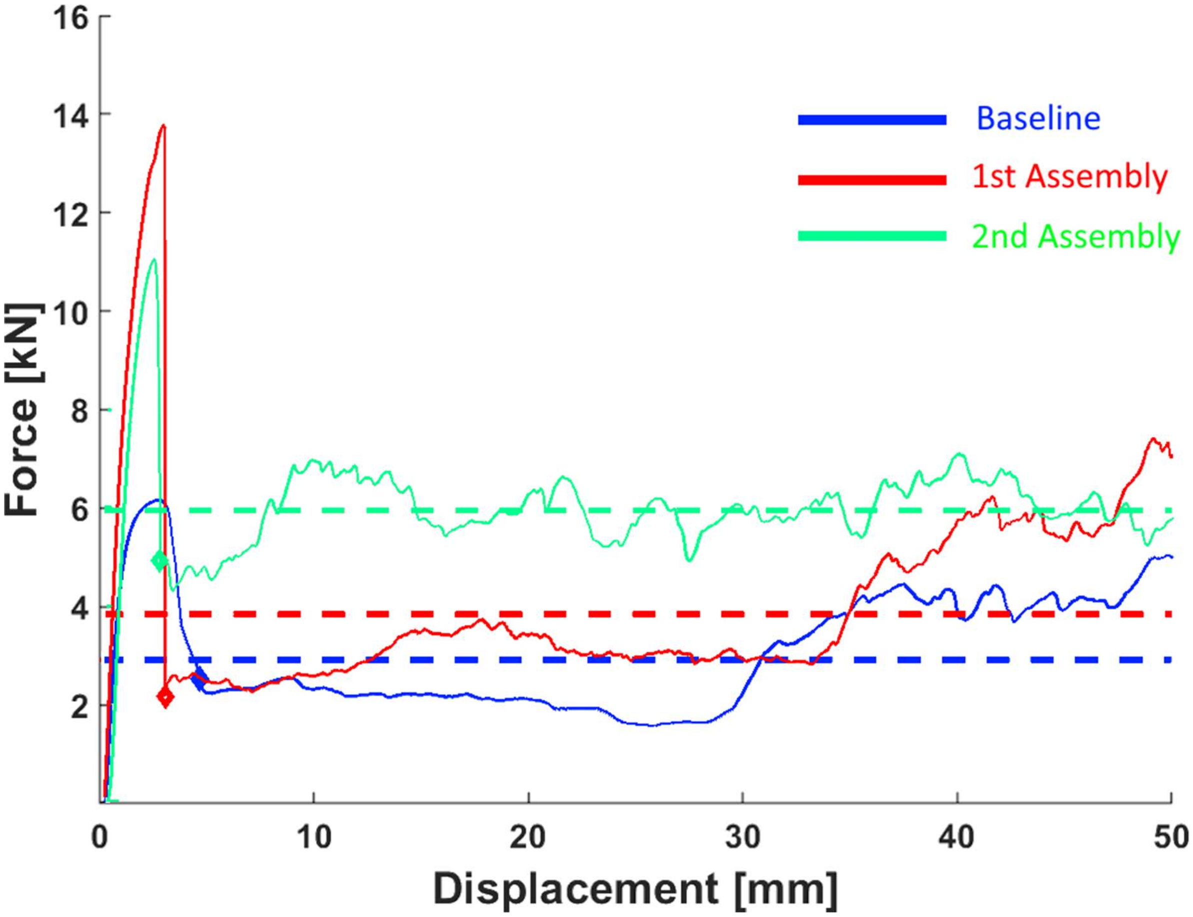

Figure 7 - Comparison between typical Force vs displacement curves of the three sets

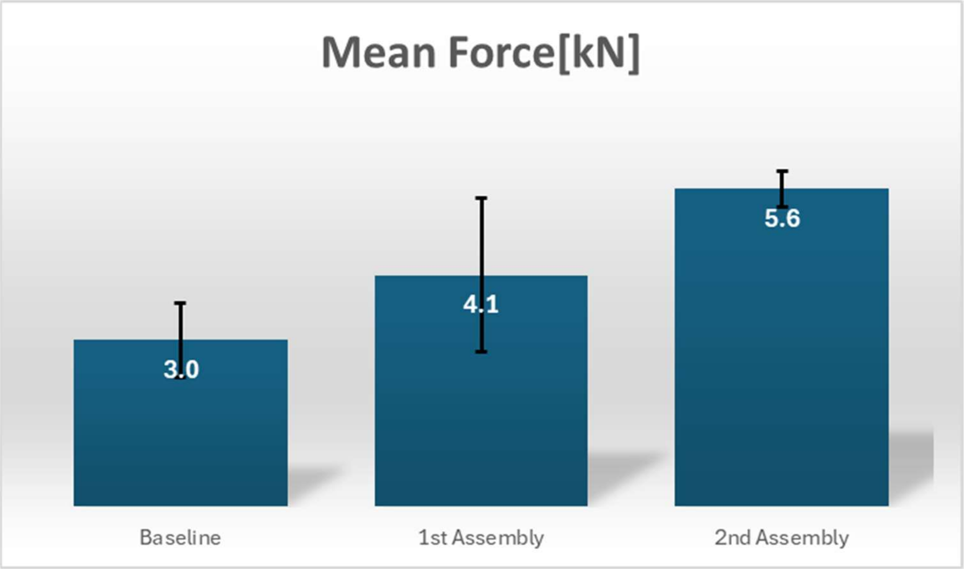

Figure 8 - Mean crush force (average values - 95% C.I.)

The above discussion is directly reflected on the force vs displacement curves compared and shown in Figure 7. In this graph, the differences in both peak forces and the crush behavior are clearly visible, highlighted by a significant mean force increase, indicated by dotted lines. Moreover, from Figure 8, where the numerical values are reported, by observing the breadth of the error bars based on the 95% C.I., it is possible to notice that the presence of the outer mesh mitigates the possible detrimental effects of production defects or potential fiber misalignments, which could cause a certain degree of data scattering.

Finally, the Specific Energy Absorption (SEA) and the crush efficiency was calculated according to the Equations (1) and (3), respectively, and results are shown in Figure 9.

The trend observed for the SEA values follows that of the mean crush force, as these two parameters are closely related, and the SEA corresponds to the area under the force vs. displacement curve during the crush. On the other hand, the crush efficiency is higher in the second assembly case as the mean force is closer to the one of the peak forces. This aspect is strongly related to the more progressive crushing behaviour of this set of samples and may positively influence the designing process.

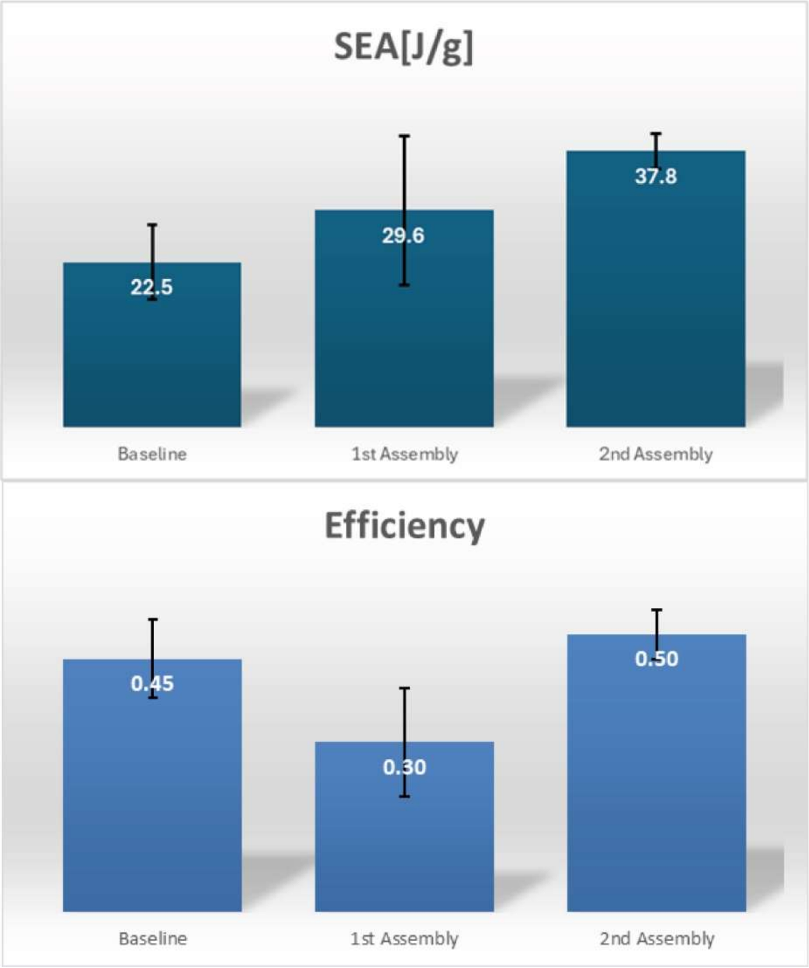

Figure 9 - Specific Energy Absorbtion (SEA) and crush Efficiency

Conclusions

In this work, the behavior of CFRP crush tubes manufactured using a custom-built desk filament winder was studied. In particular, two configurations were proposed, and results from axial crushing tests were compared with those of a baseline material. In the first configuration, an outer mesh with a 60° winding angle was co-cured with the two-layer composite tubes, with the aim of enhancing the structural stability of the thin walls, thereby promoting progressive failure and improving crush properties. In the second configuration, the same mesh was not co-cured but was instead separated by interleaving a release film. Results showed that the presence of the release film helped promote progressive failure of the tubes when subjected to axial compression. For this reason, it is believed that the proposed approach represents a promising avenue for enhancing the crashworthiness of FRP structures.

4. Contact Author Email Address

Corresponding Author: andrea.alaimo@unikore.it

5. Copyright Statement

6. Acknowledgements

This research activity has been financially supported by the Italian Ministry of University and Research (MUR) within the project DAVYD (Development of innovative technologies for control surfaces and landing gears actuation), ARS01_00940, Funding Program PNR 2015–2020.

References

[1] Savage G. Formula 1 composites engineering. *Eng Fail Anal* 2010;17:92–115.

[2] Farley, G. L. Effect of Specimen Geometry on the Energy Absorption Capability of Composite Materials. J Comp Mat, 20(4), 390–400.

[3] Palanivelu, S., Van Paepegem, W., Degrieck, J., Van Ackeren, J., Kakogiannis, D., Van Hemelrijck, D., Vantomme, J. (2010). Experimental study on the axial crushing behaviour of pultruded composite tubes. Pol Test, 29(2), 224–234.

[4] Dalli, D., Varandas, L. F., Catalanotti, G., Foster, S., & Falzon, B. G. (2020). Assessing the current modelling approach for predicting the crashworthiness of Formula One composite structures. Comp Part B, 108242.

[5] Mitsubishi Pyrofil TR 50S Datasheet

[6] IN2 Epoxy resin datasheet.

[7] Smith J, Jones B and Brown J. The title of the journal paper. *Journal Name*, Vol. 1, No. 1, pp 1-11, 2001.